

Experimental study on axial compressive behavior of hybrid FRP confined concrete columns

Li-Juan Li*, Lan Zeng, Shun-De Xu and Yong-Chang Guo

School of Civil and Transportation Engineering, Guangdong University of Technology,
100 Waihuan Xi Road, Panyu District, 510006, Guangzhou, China

(Received May 28, 2013, Revised December 13, 2016, Accepted January 10, 2017)

Abstract. In this paper, the mechanical property of CFRP, BFRP, GFRP and their hybrid FRP was experimentally studied. The elastic modulus and tensile strength of CFRP, BFRP, GFRP and their hybrid FRP were tested. The experimental results showed that the elastic modulus of hybrid FRP agreed well with the theoretical rule of mixture, which means the property of hybrid composites are linear with the volumes of the corresponding components while the tensile strength did not. The bearing capacity, peak strain, stress-strain relationship of circular concrete columns confined by CFRP, BFRP, GFRP and hybrid FRP subjected to axial compression were recorded. And the confinement effect of hybrid FRP on concrete columns was analyzed. The test results showed that the bearing capacity and ductility of concrete columns were efficiently improved through hybrid FRP confinement. A strength model and a stress-strain relationship model of hybrid FRP confined concrete columns were proposed. The proposed stress-strain model was shown to be capable of providing accurate prediction of the axial compressive strength of hybrid FRP confined concrete compared with Teng *et al.* (2002) model, Karbhari and Gao (1997) model and Miyachi *et al.* (1999) model. The modified stress-strain model was also suitable for single FRP confinement cases and it was so concise in form and didn't have piecewise fitting, which would be easy for use in structural design.

Keywords: hybrid FRP; confined concrete column; axial compressive test; mechanical behavior; stress-strain model

1. Introduction

The superior material properties of the fiber reinforced polymer (FRP) composite materials, such as light weight, high strength, good corrosion resistance, make them very suitable for strengthening a broad range of structural members, including beams, columns, slabs and walls. As a result, the past decade has witnessed the fast development of research on the use of FRP materials in civil engineering (Teng *et al.* 2002, Saadatmanesh and Ehsani 1991, Sundararaja and Prabhu 2012, Chen *et al.* 2012, Guo *et al.* 2012, Teng *et al.* 2012). It is universal to apply one type of FRP materials, such as carbon fiber reinforced polymer (CFRP), glass fiber reinforced polymer (GFRP), or basaltic fiber reinforced polymer (BFRP) to strengthen concrete columns, and their advantages and disadvantages of application are obvious (Meier *et al.* 1993, Guo *et al.* 2009, Mosallam *et al.* 2012, Rousakis and Karabinis 2012). For instance, CFRP can improve the bearing capacity of members effectively with its high elastic modulus and tensile strength, but it also has a relatively high cost price and low elongation which results in the poor deformation performance of reinforced structures. On the contrary, GFRP is low in strength and elastic modulus, but it has much higher elongation and lower prices, which increases the ductility of the strengthened structures while decreases

their cost. The material of BFRP, as a newly developed FRP material, has a higher strength and elastic modulus than GFRP, and a much lower cost price than CFRP, which has a very promising application on structural reinforcement. Recently, a number of studies about FRP strengthening method are focused on hybrid strengthening program, in which different FRP materials are used to achieve expected strengthening results (Chen *et al.* 2008, Li *et al.* 2009, Vanaja and Rao 2002, Mahdikhani *et al.* 2016), or to obtain FRP confined new members (Guo *et al.* 2009, Li *et al.* 2016).

The studies on using hybrid fiber reinforced polymer (HFRP) that is combined with different types of FRP to strength concrete members have been mainly focused on HFRP strengthened concrete beams and columns (Li *et al.* 2009, Lau and Pam 2010, Djeddi *et al.* 2016, Padanattil *et al.* 2017). Hosny *et al.* (2006) found that a single type of FRP can enhance the load-bearing capacity of T-beam strengthened but lower its ductility, while a hybrid use of CFRP and GFRP can improve both the load-bearing capacity and ductility of the strengthened beams. Moreover, Li *et al.* (2002) studied the behavior of beam-column joints strengthened with FRP and found that HFRP can improve both the stiffness and load-bearing capacity of the concrete counterparts, absorb deformation energy and postpone the appearance of concrete cracks. The studies of Bouchelaghem *et al.* (2011) and Zhao *et al.* (2013) pointed out that hybrid use of FRPs can effectively increase the load-capacities of the strengthened members, meanwhile increase the ductility of members and thus achieve an optimum use of the materials.

*Corresponding author, Professor
E-mail: lilj@gdut.edu.cn



(a) Specimen un-wrapped



(b) Specimen wrapped

Fig. 1 Specimen columns

A thorough review of related existing literature reveals that the studies on compressive behavior of HFRP confined concrete structures (especially columns) are quite limited. Due to the improving ductility of strengthened members which can be obtained with HFRP, the HFRP confined concrete has a special potential to be used in the structures with seismic resistance requirements. The stress-strain relationship of HFRP confined concrete columns is necessary in the aseismic design of structures. Different stress-strain models of FRP confined concrete materials were proposed (Farids and Khalili 1982, Miyauchi *et al.* 1999, Su *et al.* 2016 and Samaan *et al.* 1998), among which the model proposed by Teng *et al.* (2002) had been accepted by many researchers as a recommended model. Nevertheless, whether the existing models of FRP confined concrete can be extended to predict the behavior of HFRP confined concrete is yet to be confirmed.

Against above background, this paper presents an experimental study on concrete columns confined by three kinds of hybrid FRPs, including CFRP, BFRP and GFRP, with the main aim of study being exploring the confinement effect of the hybrid use of FRPs on concrete. The compressive strengths and stress-strain curves of concrete columns confined by HFRP were presented, based on the performance of FRPs which was demonstrated, and a stress-strain model of the concrete confined by HFRP was proposed as well.

2. Test specimens

2.1 Design of specimens

In this study, 30 cylinder specimens, including 27 cylinders wrapped by FRP and the other three unwrapped, with a diameter of 150 mm and a height of 300 mm were cast for testing as shown in Fig. 1. The average cube compressive strength of concrete was 38.73 MPa. The

Table 1 Mechanical properties of FRPs

Type of FRP	Tensile strength (MPa)	Elastic modulus (GPa)	Elongation (%)	Thickness (mm)	Surface density (g/m ²)	Cost price (yuan/m ²)
CFRP	4833	254.16	1.71	0.167	300	140
BFRP	1575	83.98	2	0.153	285	35
GFRP	1079	69.45	2.23	0.111	280	9

Table 2 Details of specimens

Specimen	Fiber wrapping approach	Numbers of specimen	Types of FRP
P0	None	3	—
C2	Two layers of CFRP	3	1
B2	Two layers of BFRP	3	1
G2	Two layers of GFRP	3	1
C1B1	One layer of CFRP/One layer of BFRP	3	2
C1B2	One layer of CFRP/Two layers of BFRP	3	2
C1G1	One layer of CFRP/One layer of GFRP	3	2
C1G2	One layer of CFRP/Two layers of GFRP	3	2
B1G1	One layer of BFRP/One layer of GFRP	3	2
C1B1G1	One layer of CFRP/One layer of BFRP/One layer of GFRP	3	3

Note: P0 refers to the normal concrete specimen, while B, G and C refer to BFRP, GFRP and CFRP respectively. C1B1 means that the specimen is wrapped by one layer of CFRP and one layer of BFRP from inner to outside, and the names of other specimens comply with the same rule

molds of specimens were removed in 24 hours after pouring, and the specimens were cured in a standard curing room for 28 days before testing, then the specimens were wrapped with HFRP, including CFRP, BFRP and GFRP. The related material properties of the three FRPs were measured by testing and shown in Table 1. The impregnated epoxy resin was used as the adhesive. From the statistics provided by the manufacture, the tensile strength, elastic modulus and elongation were above 40 MPa, 2500 MPa and 1.5%, respectively.

2.2 Wrapping and testing method

The method of wet layup was applied to wrap the plain concrete column with the fiber sheet and epoxy resin. Firstly, the FRP sheet should be cut into a regular size with a width of 300 mm. Before wrapping the plain concrete, the loose dust on the concrete surface should be removed by a grinding wheel and the holes in the concrete should be filled with plaster to provide a better condition for bonding FRP sheet. Then, the adhesive made by mixing compositions A and B of epoxy resin in a volume ratio of A:B=1:1 was first uniformly covered to the surface of concrete columns and layers of pre-impregnated CFRP was then attached along the hoop direction of the specimens. The ratio of fiber is basically above 80% in volume for three types of FRP. The overlapping length was set as 150 mm in hoop direction and the overlapping zones were deliberately offset from layer to layer. At last, two layers of CFRP with 50 mm width were wrapped on the two ends of the HFRP confined column in order to prevent local compressive failure near the ends of

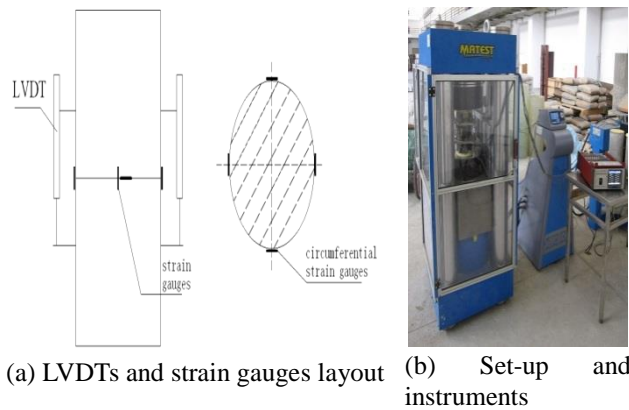


Fig. 2 Arrangement of measure points and loading

columns. Before loading, both ends of the specimens were leveled by super-strength gypsum.

Details of specimen are shown in Table 2. For HFRP confined columns, the order of the type of FRP from inside to outside was arranged according to the elongation of the fiber. Since the fiber inside has a smaller hoop strain compared with the outer fiber, the inner fiber ranked with lower elongation is expected to have better bearing capacity and ductility.

Four strain gauges were bonded uniformly on the specimens in longitudinal and hoop directions to record the strains in the two directions respectively. In addition, axial strains were also measured by two linear variable displacement transducers (LVDTs) at 180° apart and covering the mid-height region of 120 mm for both unconfined and confined specimen, as is shown in Fig. 2(a). The loading was applied by MATEST material testing machine made in Italy, with a displacement control of 0.18 mm per minute, as is shown in Fig. 2(b).

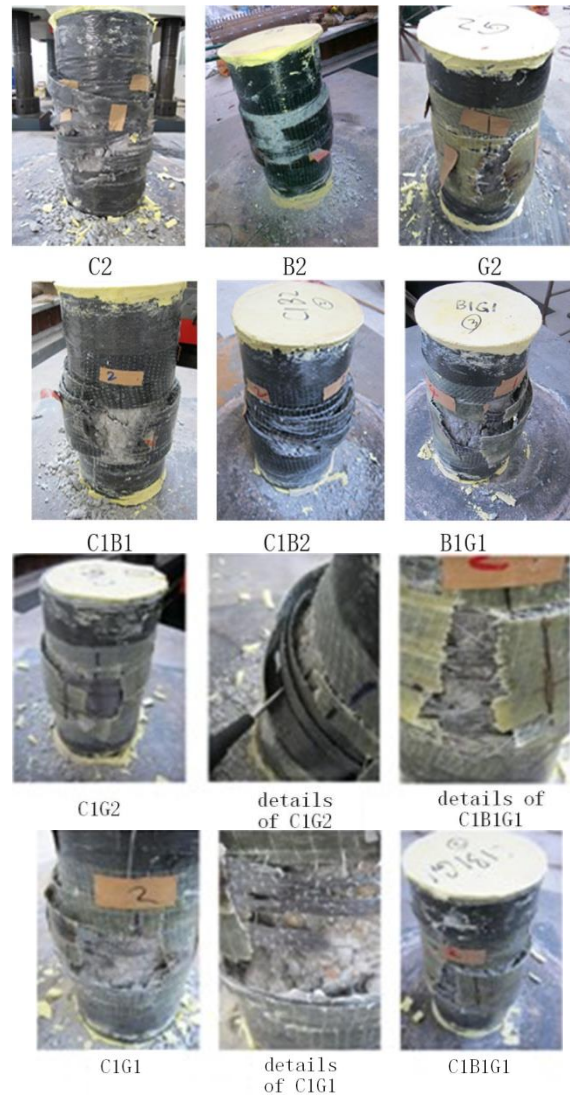


Fig. 3 The failure modes of specimens

3. Test results and analysis

3.1 The failure modes

Sounds arising from FRP rupture could be heard from time to time when the confined concrete columns were loaded to about 80% of its ultimate load-bearing capacity. It can be observed that the rupture of FRP increased with the increase of loads, till the ultimate compressive failure of the confined specimens.

When the failure of columns confined by CFRP occurred, the FRP sheet was quickly fractured into strips, which was accompanied with a loud popping sound and a sharp decrease of the load-bearing capacity, suggesting a typical brittle fracture. Compared with the concrete columns confined by CFRP, cracking sound heard during the failure process of the columns confined by BFRP is smaller, which was accompanied by a quick drop of the load-bearing capacity. During the failure process of the concrete columns confined by GFRP, there was no apparent sound arising from FRP rupture (due to the large deformation behavior of GFRP). Instead, the central part of the specimen bulged, leading to the appearance of a number of parallel small cracks on the GFRP sheet; the cracked GFRP region was

eventually extended towards to the two ends of columns till rupture of GFRP appeared. The above failure process was quite progressive. So, it can be said that the failure of GFRP confined columns is much more ductile than those confined by CFRP and BFRP.

For the concrete columns confined by one type of FRP (CFRP/BFRP/GFRP), the fracture of FRP usually happened around the middle region of the column. On the other hand, for the concrete columns confined by HFRP, the fibers were tore apart to some extent when fractured, indicating an obvious ductility failure. The failure modes of specimens were shown in Fig. 3.

For the circular concrete columns confined by HFRP, the inner fiber is ruptured firstly because of its lower elongation, which was easier to reach the rupture strain under the same loading. The fibers of higher elongation help to prevent cracks in concrete from propagation and carry the additional loads caused by the fracture of the fibers of lower elongation. As a result, a kind of parallel cracks formed within the FRP sheet with higher elongation. Meanwhile, the stress released from the damaged inner layer fibers was transformed to the outer one via the

Table 3 Key experimental results and their comparison

Specimen	Load-bearing capacity (MPa)	Relative value	Longitudinal strain	Relative value	Hoop strain	Relative value	Strengthening cost (yuan)	Relative cost performance
P0	31.72	1.00	3017	1.00	2118	1.00	—	—
C2	92.87	2.93	27937	9.26	11173	3.70	70.69	1.00
G2	47.63	1.50	10805	3.58	12252	4.06	31.55	1.15
B2	57.29	1.81	13403	4.44	12254	4.06	21.86	1.99
C1G1	74.19	2.34	20277	6.72	13870	4.60	46.28	1.22
C1G2	83.81	2.64	21569	7.15	14088	4.67	54.66	1.17
C1B1	74.73	2.36	20597	6.83	12551	4.16	51.12	1.11
C1B2	87.77	2.77	24000	7.95	13106	4.34	64.36	1.04
B1G1	53.12	1.67	12153	4.03	11990	3.97	26.71	1.51
C1B1G1	75.56	2.38	20153	6.68	12869	4.27	59.51	0.97

Note: The strengthening cost includes the cost of fiber sheet and the epoxy resin covered with the concrete and the fiber sheet. The cost of epoxy resin is calculated as 36 yuan/m³

concrete members, which increases the stress of outer fiber. At last, the outer fibers fractured at their weakest section. The different elongations of fibers within the HFRP prevent the sudden rupture of the HFRP as a whole, leading to a progressive rupture process of the HFRP. As a result, the failure of the columns confined with HFRP is generally more ductile than those confined by a single type of FRP.

3.2 Analysis of compressive strength, fiber performance and ductility

The load-bearing capacity, hoop and axial strains of concrete columns measured in the test were shown in Table 3.

Compared with control specimen P0 (without FRP confinement), the compressive strengths of specimens with two layers of fibers, namely C1G1, C1B1 and B1G1 are increased by 134%, 136% and 67% respectively (see Table 3). The compressive strength of C1G1 and C1B1 are nearly the same, but the hoop strain of FRP in C1G1 is obviously bigger than that in C1B1, which suggests that if the combination of fiber elongations is appropriate, the confined specimen can take the advantage of the fiber with high elongation and decrease the brittleness of specimens failure caused by rupture failure of FRP, which makes full use of the elongations of different fibers and increases the deformation capacity of specimens. Moreover, the strengthening cost of C1G1 is about 11% less than that of C1B1, so the hybrid effect is economically enhanced by the combination of CFRP and GFRP rather than that of CFRP and BFRP for confining concrete columns.

The strengths of concrete columns confined by three-layer of FRP are higher than that by two-layer. Moreover, the compressive strength of C1G2 and C1B2 is higher than that of C1B1G1; the latter is higher than that of C1B1 only by 1.57 MPa with an increasing strengthening cost up to 16%. This again suggested that the combining application of FRPs has a significant effect on the strength of specimens, but the confinement effect and the cost performance will not be significantly increased with the

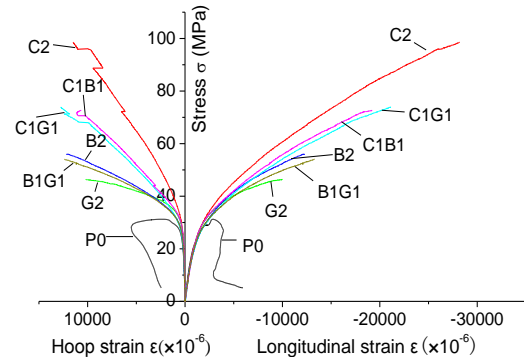


Fig. 4 Stress-strain curves of specimens with 2 layers of FRP

increase of fiber types. It also suggested that three kinds of fibers (or more) may be not suitable to be used together in practice.

The hoop strains of C2, G2 and B2 are 1.11%, 1.23% and 1.22% respectively when FRP rupture happened, while the hoop strains of C1G1 and C1B1 are 1.39% and 1.26%, obviously higher than those of single type fiber (such as C2, G2 and B2), also suggesting that hybrid use of FRPs can make a full use of the high elongation property of some FRP (e.g., GFRP) to enhance the ductility of specimens. However, the hoop strain of B1G1 is lower than those of B2 and G2. A possible explanation is that the elongation gap between the two types of FRPs (BFRP and GFRP) is so small that the confinement of HFRP for concrete columns hasn't taken into full play; on the contrary, some detrimental effects caused by pestering and overlapping between layers of fibers may be triggered and exaggerated. Thus, the influence of hybrid effect needs to be further studied. The hoop strains of the concrete columns confined by three-layer of HFRP, such as C1G2 and C1B2 are higher than that by two-layers, such as C1G1 and C1B1 indicating that with the increase of layers of FRP with higher elongation, the hybrid effect can be fully developed and the ductility of concrete columns confined by HFRP can be improved.

The relative cost performance was calculated from the ratio of strengthening cost to load-bearing capacity compared with that of specimen C2. The value of relative cost performance for C1G1 (1.22) is higher than both values for C2 (1.0) and G2 (1.15), which means Hybrid FRP is able to improve the bearing capacity of concrete columns better than single FRP without adding strengthening cost. However, among layers of HFRP confined concrete columns, the value of relative cost performance for C1G2 (1.17) is lower than that for C1G1 (1.22), and the value for C1B2 (1.04) is C1B1 (1.11), which means on the promise of safe bearing capacity, decreasing the layers of HFRP tends to improve the cost performance.

3.3 Effects of FRP layers on stress-strain curves

Stress-strain curves of all specimens are shown in Figs. 4-5. The axial strain is calculated from the readings of LVDT (the average of reading from the two LVDTs), while the hoop strain is calculated by the average value of axial

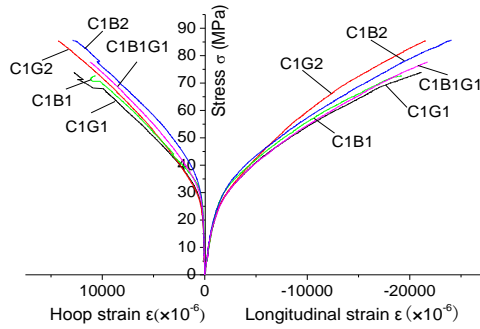


Fig. 5 Stress-strain curves of specimens with 3 layers of FRP

strains from the strain gauges.

It can be seen from Fig. 4 that, compared with columns without FRP (i.e., specimen P0), the stress-strain curves of circular concrete columns confined by FRP are nearly the same when the hoop strain is smaller than peak strain of P0 (strain corresponding the peak strain). The hoop strain of concrete is small before reaching peak strength and will increase greatly after the peak point. This is mainly because, before peak point, the hoop expansion of concrete was very slight (only resulting from Poisson’s effect), and thus the confinement effect of FRP could not be acted. For the FRP confined concrete column, when the stress can be increased considerably above the peak strength of P0, but the slopes of stress-strain curves (both hoop strains and axial strains) decrease sharply, which are much lower than those of the first segment. As reported (Teng *et al.* 2002), the curves of the second segment are nearly linear; the slopes of the curves in the second segment are affected by the stiffness of HFRP; and the stress magnitude for the intersection point of the extension line of the second segment of curves with the stress axis is close to the peak strength of P0.

For the concrete columns confined by 2 layers of FRP, the slopes of axial strain are nearly the same. That is to say, the trends of axial strain are similar, but the slopes of hoop strain are significantly different, with trends being affected by the types of hybrid fibers. The stiffness of the axial strain in the reinforced segment can be divided into four groups: (1) C2, (2) C1B1 and C1G1, (3) B2 and B1G1, (4) G2. The slopes of the hardening segment of the stress-strain curves decrease from the first group to the fourth group, but the difference is very slight. As to the stress-axial strain curves of columns confined by HFRP, the stiffness in the hardening segment is determined mainly by the fiber of low elongation, but affected by fiber of the high elongation, which is mainly due to the fact that among the FRPs used in this study, FRP with lower elongation has higher confinement stiffness (in proportional to $E_f t_f$).

It can be seen from Fig. 5 that compared with the columns confined by 2 layers of FRP (C1B1 and C1G1), the stiffness of the columns confined by 3 layers of FRP (C1G2 and C1B2) on the hardening segment is apparently increased, showing that confinement effect can be improved by increasing confining FRP layer. However, compared with that of C1B1, the slope in the hardened segment of C1B1G1 is nearly not increased, which indicates that the

Table 4 Confinement stiffness of HFRP

Specimen	C2	B2	G2	C1B1	C1B2	C1G1	C1G2	B1G1
Calculation stiffness $\times 10^{12}$ (N/m)	54.18	16.40	9.79	35.29	43.49	31.94	36.95	13.09

increase of the types of FRPs may not have a significant contribution on the confinement. To clarify the reasons for the above complex needs further research.

As for stress-hoop strain curves of columns confined by HFRP, the stiffnesses in the hardening segment are various. It can be seen from Fig. 5 that the hoop stiffness can be sorted as $C1B2 > C1B1G1 > C1G2 > C1B1 > C1G1$ when confinement increased from 2-layer to 3-layer, which matched the order of the confinement stiffness of FRP well.

From the above discussions, it can be concluded that the load-bearing capacity of circular concrete columns confined by HFRP is mainly controlled by the FRPs of low elongation, while the FRPs with high elongation helps to enhance the ductility of columns, thus reduces the speed of development of the hoop strain in the hardening segment and postpones the failure of the specimen.

3.4 Effects of stiffness on stress-strain curves

The performance of specimens in the reinforced segment is affected by the stiffness of hoop strain. The confinement stiffness is defined as

$$K = \frac{\Delta F}{\Delta L} \tag{1}$$

where K is the stiffness, and ΔF and ΔL is the increment of force and displacement respectively. Eq. (1) can be rewritten as

$$K = \frac{\Delta F}{\Delta L} = \frac{\frac{\Delta F}{A} A}{\frac{\Delta L}{L} L} = E \frac{th}{L} \tag{2}$$

where, A is the cross-sectional area of the column confined by HFRP, L is the length of HFRP, which is regarded as the circumference of specimen approximately, t is the thickness of HFRP, h is height of constraint fibers, which is the same as that of the column, E is the elastic modulus of HFRP.

The confinement stiffness of each group of HFRP can be calculated by Eq. (2), and shown in Table 4.

It can be seen from Table 4 that the differences in confinement stiffness of group B1G1 and B2, group C1G1 and C1B1, group C1B1G1 and C1B2 are 3.31, 3.35 and 3.33 respectively. The differences of constraint stiffness are very small. The stress-strain curves of the three groups of specimens are shown in Figs. 6-8. The maximum difference of confinement stiffness is 44.39 and is that between C2 and G2. The stress-strain curves of this group of specimens are shown in Fig. 9.

The circular concrete columns have hoop expansion under compression, and their expansion is restricted by FRP. So under the same hoop constraint, the longitudinal

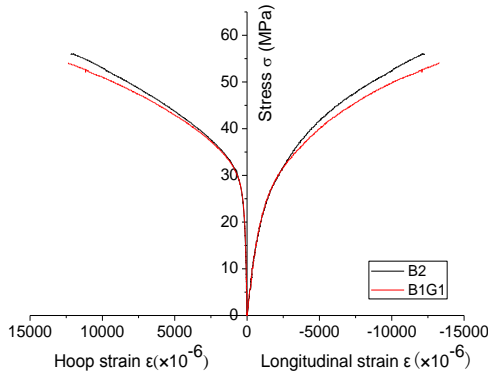


Fig. 6 Stress-strain curves of B2 & B1G1

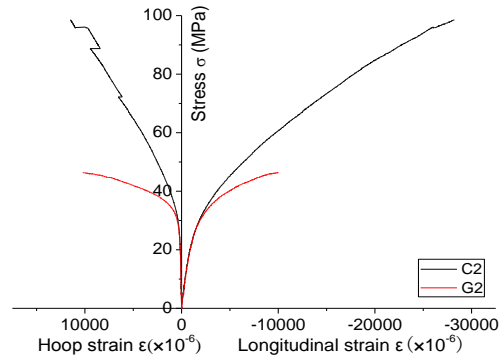


Fig. 9 Stress-strain curves of C2 & G2

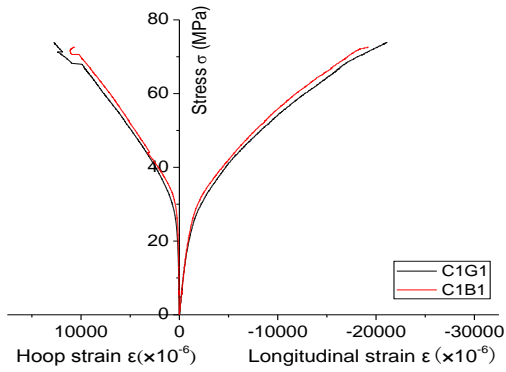


Fig. 7 Stress-strain curves of C1G1 & C1B1

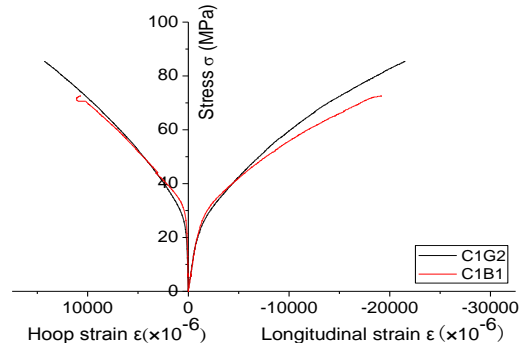


Fig. 10 the Stress-strain curves of C1B1 & C1G2

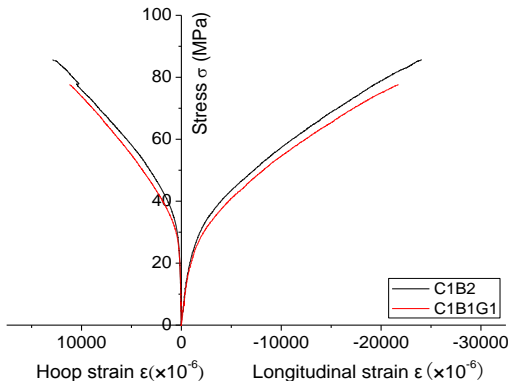


Fig. 8 Stress-strain curves of C1B1G1 & C1B2

strain and stress of concrete columns are the same, and the only difference lies in the rupture strengths of fibers, which are directly related with the ultimate compressive strength of circular concrete columns.

It can be seen from Figs. 6-7 that the slopes of stress-strain curves in the hardening segment are almost the same if the difference in confinement stiffness of HFRP is small. However, the compressive strength of confined concrete is different. It can be seen from Fig. 9 that the slopes of the curves in the second segment are obviously different if the confinement stiffness of HFRP varies greatly, which indicates that the slopes of the curves in second segment, namely the hardening segment, are mainly affected by confinement stiffness of HFRP. For example, the difference of the confinement stiffness between C1B1 and C1G2 is only 1.66, so the slopes of their hardening segments are nearly the same, as shown in Fig. 10. The small difference

of slop in the later stage can be attributed the higher elongation of the GFRP, which was proved by comparing the hoop fracture strain of the two specimens. So, it can be said that the stress-strain relation curves in the second segment are affected by the elongation capacity of the outer FRP layer which has a significant bearing on the hoop constraint in FRP.

4. Stress-strain model

4.1 Determination of HFRP parameters

The existing studies (Hai and Mutsuyoshi 2012, Rousakis and Karabinis 2012, Mosallam *et al.* 2012) suggest that the elastic modulus of HFRP is agree well with the theory of mixture, and the equation is as follows.

$$E = E_1V_1 + E_2V_2 + E_3V_3 \tag{3}$$

where E is the elastic modulus, V is the volume fraction of fibers with its subscript representing the fiber type. The subscript numbers 1, 2 and 3 refer to the type of CFRP, GFRP and BFRP respectively.

The elastic modulus of HFRP can be calculated by Eq. (3), and the comparison between the calculated and measured values are shown in Table 5. It can be seen that Eq. (3) provides rather good predictions on the experimental values of elastic modulus for HFRP.

The hoop tensile strength of HFRP f_{frp} cannot be calculated by the theory of mixture, but it can be calculated exactly by the coefficient of hybrid effect (Xu 2012), as follows.

Table 5 Elastic modulus of HFRP

Specimen	C1B1	C1B2	C1G1	C1G2	B1G1	C1B1G1
Measured elastic modulus (GPa)	172.85	143.41	193.68	165.91	96.27	159.41
Calculated elastic modulus (GPa)	172.79	144.06	180.4	149.13	77.87	146.18

Table 6 Elastic modulus, lateral constraint and failure strength of HFRP

Specimen	E (GPa)	φ	V_{le}	R_e	f_{frp} (MPa)	f_l (MPa)
C2	254.16	—	—	—	4833.50	21.53
B2	83.98	—	—	—	1575.90	6.43
G2	69.45	—	—	—	1175.60	3.48
C1B1	172.79	0.50	0.522	0.2390	2196.53	9.37
C1B2	144.06	0.33	0.353	0.2135	1793.64	11.31
C1G1	180.40	0.50	0.600	0.2000	2221.08	8.23
C1G2	149.13	0.33	0.430	0.1881	1817.88	9.43
B1G1	77.87	0.50	0.580	0.2100	966.72	3.40
C1B1G1	146.18	0.33	0.353	0.2135	1820.03	10.46

Table 7 Strength obtained from simulation models and experimental results

Specimen	Test strength (MPa)	This paper's model	Teng <i>et al.</i> (2002) model	Karbhari and Gao (1997) model	Miyauchi <i>et al.</i> (1999) model
		$k_1=4.88$	$k_1=2$	$k_1 = 2.1(\frac{f_l}{f_{co}})^{0.13}$	$k_1=2.98$
C1B1	73.99	77.45	50.46	54.78	59.65
C1B2	87.77	86.92	54.34	58.88	65.43
C1G1	74.19	71.9	48.19	52.32	56.25
C1G2	83.81	82.91	52.70	57.16	62.98
B1G1	53.12	50.71	38.53	41.27	41.86
C1B1G1	75.56	82.76	52.64	57.09	62.89

$$f_{frp} = E\varepsilon_{le}(1 + R_e)S \quad (4)$$

where, E is the elastic modulus of HFRP. ε_{le} is the ultimate elongation of the FRPs with lower elongation. S is the correction factor to account for the difference between the hoop tensile strength and tensile strength, taken as 0.6; R_e is a hybrid factor and calculated by following formulation

$$R_e = T^2\varphi(1 - V_{le}) \quad (5)$$

where T is the wrapping coefficient related to the wrapping approach of layers, and is taken as 1 when hybrid layers were used. φ is the dispersion coefficient. V_{le} is the volume fraction of the fibers of lower elongation.

The horizontal expansion takes place in the concrete when concrete columns confined by FRP are under axial compression. The expansion is constrained by FRP, whose confinement effect is affected by the quantity and intensity of FRP as well as the diameter of confined columns, expressed as follows

$$f_l = \frac{2f_{frp}t_{frp}}{d} \quad (6)$$

Table 8 Statistical indexes of strength model in this paper

Model	Ratio of test and calculation values		
	Average	Standard deviation	Variation coefficient (%)
Simulation model of this paper	1.016	0.068	6.7
Teng <i>et al.</i> (2002) model	1.517	0.104	6.8
Karbhari and Gao (1997) model	1.144	0.061	5.3
Miyachi <i>et al.</i> (1999) model	1.297	0.071	5.5

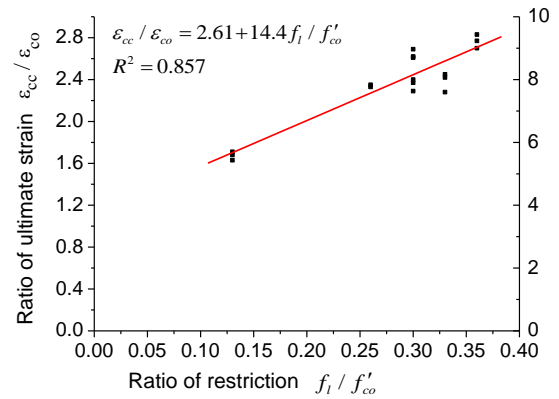


Fig. 11 Regression of ultimate axial strain for concrete confined by HFRP

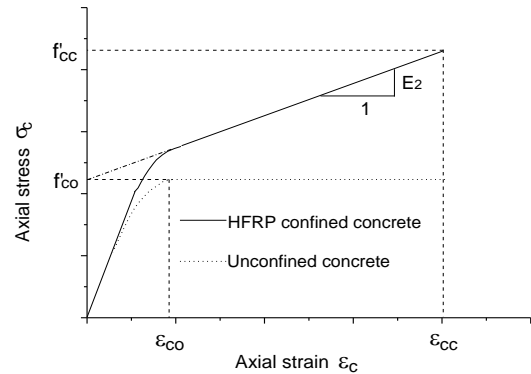


Fig. 12 Stress-strain relationship of concrete confined by HFRP

where, t_{frp} is the calculated thickness of FRP, d is the diameter of confined circular concrete columns.

The elastic modulus, lateral constraint and failure strength of HFRP can be calculated from Eqs. (3)-(6), and shown in Table 6.

4.2 Strength model of concrete confined by HFRP

The following strength model of confined concrete was presented by Richart (Richart *et al.* 1928) and was directly used to FRP confined concrete by Farids (Farids and Khalili 1982). It is a mostly adopted strength model of concrete confined by FRP at present and is expressed as Eq. (7) as follows

$$\frac{f'_{cc}}{f'_{co}} = 1 + k_1 \frac{f_l}{f'_{co}} \quad (7)$$

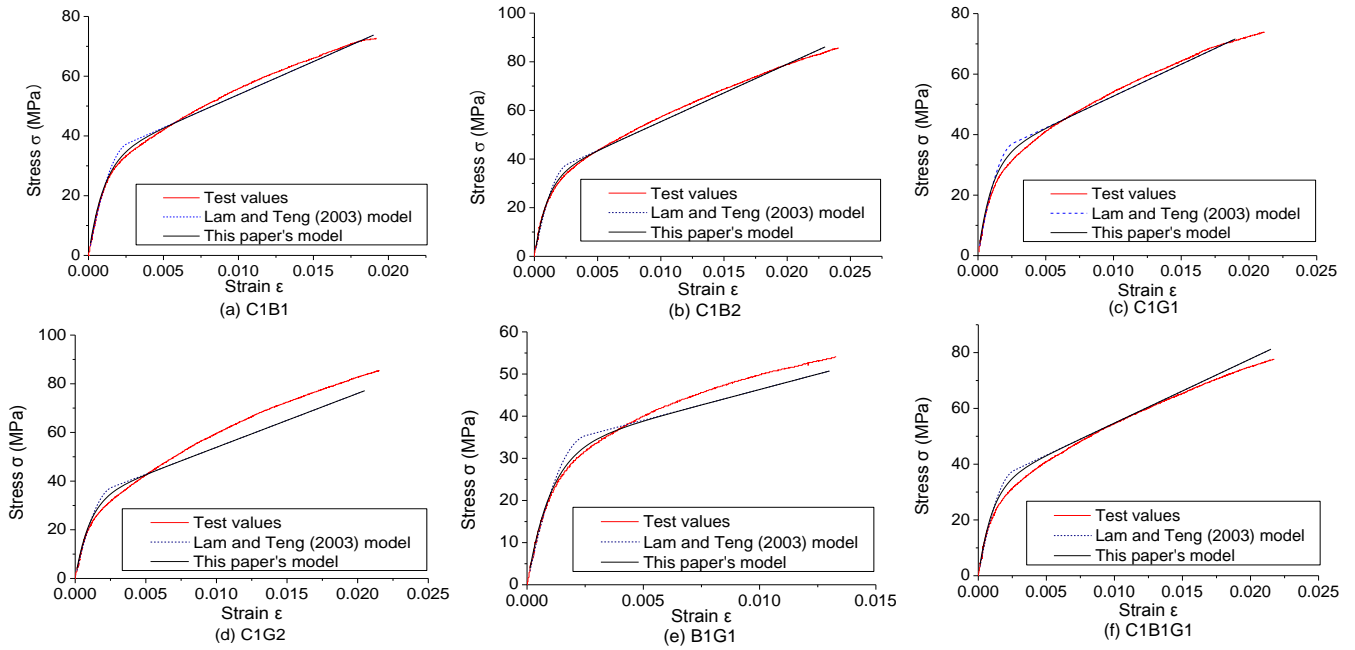


Fig. 13 Comparison of experimental curves and theoretical curves

Table 9 Correlation coefficient of test values and theoretical calculation

Specimen	This paper's model	Lam and Teng (2003) model
C1B1	0.99921	0.99759
C1B2	0.99859	0.99628
C1G1	0.99803	0.99296
C1G2	0.99575	0.98993
B1G1	0.99600	0.98266
C1B1G1	0.99830	0.99484

where, f_{cc}' and f_{co}' refers to the compressive strength of concrete confined and unconfined by FRP separately. f_l is the lateral restraint stress. k_1 is the constraint validity coefficient.

This paper takes a linear regression analysis on the experimental data, and the strength model of concrete confined by FRP is obtained as follows

$$\frac{f_{cc}'}{f_{co}'} = 1 + 4.88 \frac{f_l}{f_{co}'} \quad (8)$$

Table 7 lists the comparisons between typical strength models and the experimental strengths obtained in the present study, with the statistical indexes of typical strength models listed in Table 8. It can be obtained from Tables 7 and 8 that the strength predicted by the typical strength models is smaller than the tested ones for circular concrete columns confined by HFRP. However, the predicted strength based on Eq. (8) agrees well with the experimental value, with a correlation coefficient of 0.926, an average ratio of 1.016, a standard deviation of 0.068 and a variation coefficient of 0.067.

4.3 Ultimate axial strain of concrete confined by HFRP

The ultimate axial strain of concrete confined by HFRP is a key parameter of the stress-strain curve. The value of the parameter is related with the lateral restricting stress f_l , as shown in Fig. 11.

The relationship between dimensionless ultimate axial strain and the constraint ratio is shown in Fig. 11. It can be seen that there exists a nearly linear relationship between the ultimate axial strain and constraint ratio. The relationship can be described by the linear regression analysis and is shown by the following Eq. (9)

$$\frac{\varepsilon_{cc}}{\varepsilon_{co}} = 2.61 + 14.4 \frac{f_l}{f_{co}'} \quad (9)$$

where, ε_{cc} is the ultimate axial strain of concrete confined by FRP, ε_{co} is the ultimate axial strain of normal concrete.

4.4 Stress-strain model

Lam and Teng (2003) model was proposed based on a stress-strain relationship database collecting from former experimental researches, which was testified to agree well with the test values by many other researchers and showed a good prediction for the stress-strain relationship, and it was widely recommended in the structural design. Specifically, in the Model, the stress-strain curve of FRP confined concrete with sufficient confinement features a monotonically ascending bi-linear type. The former section consists of a parabola related to the property of unconfined concrete and the second section is a straight line related to the confinement effect with a connection smoothly. Even Lam and Teng (2003) model has an accurate evaluation on the stress-strain relationship of FRP confined concrete, it has a relatively complex format with various of parameters that need to be obtained from material tests before and the process of calculation is also complicated.

To develop a simple but accurate model for the stress-strain relationship for the concrete confined by HFRP, without using the piecewise function, two hypotheses based on the stress-strain curves which were recorded from the experimental results were taken in this paper. Firstly, the intersection point between the extension line of the hardening segment of the stress-strain curve and the stress axis equals to the compressive strength of normal concrete. Secondly, the termination point in the hardening segment expresses both the compressive strength and ultimate axial strain, as shown in Fig. 12. These two hypotheses, ignoring those assumptions of the piecewise function that were not suitable for this paper's model, were also drawn from the assumptions of Lam and Teng (2003) model.

Based on the above two assumptions, the relationship of axial stress σ_c with axial strain ε can be proposed as Eq. (10) as follows

$$\sigma_c = f'_{co}(1 - e^{-1000\varepsilon}) + E_2\varepsilon, \quad (10)$$

when $0 \leq \varepsilon \leq \varepsilon_{cc}$

where, E_2 is the slope of the curve in second segment.

Based on the first assumption, the following Eq. (11) can be obtained from Fig. 12

$$E_2 = \frac{f'_{cc} - f'_{co}}{\varepsilon_{cc}} \quad (11)$$

Comparisons between the stress-strain relations predicted by the theoretical calculation and the test results are presented in Fig. 13. It can be seen from Fig. 13 that The curves calculated from the Lam and Teng (2003) model and this paper's model are similarly coincided with the curves recorded from experimental results. Compared with Lam and Teng (2003) model, the curves obtained from the model proposed in this paper is even more approached to the test ones, especially around the intersection of two segments where the calculated values from this paper's model are just slightly over estimated the test values.

The correlation coefficient of the test values and the theoretical values calculated by the paper's model and Lam and Teng (2003) model are listed in Table 9. Although the predicted values from both models are quite correlated to the experimental results, the correlation coefficient of the test values and the theoretical values calculated by this paper's model is even higher, very close to 1, which shows a better correlation to the test results.

5. Conclusions

This paper first presented an experimental study on the concrete column confined by HFRP. Based on the test results, a modified model was developed to quantitatively describe the stress-strain relationship of the concrete confined by HFRP. From the test results, discussions and comparisons presented in the present study, the follow conclusions can be drawn:

- Hybrid use of FRPs can improve the ductility of the concrete confined by FRP subjected to compression load. The rupture strain of hybrid FRP confined concrete columns

can be obviously improved than that of single fiber confined columns. The failure of columns can be delayed by reducing the speed of the development of hoop strain. On the other hand, the stiffness of circular concrete columns confined by HFRP can be improved by taking the advantage of the large stiffness of carbon fibers.

- The stress-strain model of concrete confined by HFRP presented in this paper matches the experimental results well. It is clearly aware that the model has been substantiated only against very limited test data, so much more test data are required for the improvement/validation of the proposed model.

- When three kinds of FRPs were used to confine concrete, the hybrid effect is reduced, suggesting that there should be a limitation on the number of types of FRPs used in the HFRP.

Acknowledgments

This research was funded by the National Natural Science Foundation of China (Project Nos. 51278132, 11472084) and the Foundation of Guangdong Provincial Transportation Department (Project No. 2012-04-013). The foundations are greatly appreciated.

References

- Bouchelaghem, H., Bezazi, A. and Scarpa, F. (2011), "Compressive behaviour of concrete cylindrical FRP-confined columns subjected to a new sequential loading technique", *Compos. Part B-Eng.*, **42**(7), 1987-1993.
- Chen, G.M., Chen, J.F. and Teng, J.G. (2012), "Behaviour of FRP-to-concrete interfaces between two adjacent cracks: A numerical investigation on the effect of bondline damage", *Constr. Build. Mater.*, **28**(1), 584-591.
- Chen, Z.F., Wan, L.L. and Lee, S. (2008), "Evaluation of CFRP, GFRP and BFRP material systems for the strengthening of RC slabs", *J. Reinf. Plast. Compos.*, **27**(12), 1233-1243.
- Djeddi, F., Ghernouti, Y., Abdelaziz, Y. and Alex, L. (2016), "Strengthening in flexure-shear of RC beams with hybrid FRP systems: Experiments and numerical modeling", *J. Reinf. Plast. Compos.*, **35**(22), 1642-1660.
- Farids, M.N. and Khalili, H. (1982), "FRP-encased concrete as a structural material", *Mag. Concrete Res.*, **34**(121), 191-202.
- Guo, Y.C., Huang, P.Y., Yang, Y. and Li, L.J. (2009), "Experimental studies on axially loaded concrete columns confined by different materials", *Key Eng. Mater.*, **400**(10), 513-518.
- Guo, Y.C., Li, L.J., Chen, G.M. and Huang, P.Y. (2012), "Influence of hollow imperfections in adhesive on the interfacial bond behaviors of FRP-plated RC beams", *Constr. Build. Mater.*, **30**(5), 597-606.
- Hai, N.D. and Mutsuyoshi, H. (2012), "Structural behavior of double-lap joints of steel splice plates bolted/bonded to pultruded hybrid CFRP/GFRP laminates", *Constr. Build. Mater.*, **30**(5), 347-359.
- Hosny, A., Shaheen, H., Abdelrahman, A. and Elafandy, T. (2006), "Performance of reinforced concrete beams strengthened by hybrid FRP laminates", *Cement Concrete Compos.*, **28**(10), 906-913.
- Karbhari, V.M. and Gao, Y. (1997), "Composite jacketed concrete under uniaxial compression-verification of simple design

- equations”, *J. Mater. Civil Eng.*, **9**(4), 185-193.
- Lam, L. and Teng, J.G. (2003), “Design-oriented stress-strain model for FRP-confined concrete”, *Constr. Build. Mater.*, **17**(6-7), 471-489.
- Lau, D. and Pam, H.J. (2010), “Experimental study of hybrid FRP reinforced concrete beams”, *Eng. Struct.*, **32**(12), 3857-3865.
- Li, D., Du, F., Chen, Z. and Wang, Y. (2016), “Identification of failure mechanisms for CFRP-confined circular concrete-filled steel tubular columns through acoustic emission signals”, *Smart Struct. Syst.*, **18**(3), 525-540.
- Li, J., Samali, B., Ye, L. and Bakoss, S. (2002), “Behaviour of concrete beam-column connections reinforced with hybrid FRP sheet”, *Compos. Struct.*, **57**(1-4), 357-365.
- Li, L.J., Guo, Y.C., Huang, P.Y., Liu, F., Deng, J. and Zhu, J. (2009), “Interfacial stress analysis of RC beams strengthened with hybrid CFS and GFS”, *Constr. Build. Mater.*, **23**(6), 2394-2401.
- Mahdikhani, M., Naderi, M. and Zekavati, M. (2016), “Finite element modeling of the influence of FRP techniques on the seismic behavior of historical arch stone bridge”, *Comput. Concrete*, **18**(1), 99-112.
- Meier, U., Deuring, M., Meier, H. and Schwegler, G. (1993), *Strengthening of Structures with Advanced Composites, Alternative Materials for Reinforcement and Prestressing of Concrete*, Clarke, Chapman & Hall, Glasgow, Scotland.
- Miyachi, K., Inoue, S., Kuroda, T. and Kobayashi, A. (1999), “Strengthening effects of concrete columns with carbon fiber sheet”, *J. Trans. Jpn. Concrete Inst.*, **21**(2), 143-150.
- Mosallam, A., Taha, M.M.R., Kim, J.J. and Nasr, A. (2012), “Strength and ductility of RC slabs strengthened with hybrid high-performance composite retrofit system”, *Eng. Struct.*, **36**(3), 70-80.
- Padanattil, A., Karingamanna, J. and Mini, K.M. (2017), “Novel hybrid composites based on glass and sisal fiber for retrofitting of reinforced concrete structures”, *Constr. Build. Mater.*, **133**, 146-153.
- Richart, F.E., Brandtzaeg, A. and Brown, R.L. (1928), “A study of the failure of concrete under combined compressive stresses”, *University of Illinois Bulletin*, **26**, 185.
- Rousakis, T.C. and Karabinis, A.I. (2012), “Adequately FRP confined reinforced concrete columns under axial compressive monotonic or cyclic loading”, *Mater. Struct.*, **45**(7), 957-975.
- Saadatmanesh, H. and Ehsani, M.R. (1991), “RC beams strengthened with FRP plates II: Analysis and parametric study”, *J. Struct. Eng.*, **117**(11), 3434-3455.
- Samaan, M., Mirmira, A. and Shahawy, M. (1998), “Model of concrete confined by fiber composites”, *J. Struct. Eng.*, **126**(9), 1025-1031.
- Su, L., Li, X. and Wang, Y. (2016), “Experimental study and modelling of CFRP-confined damaged and undamaged square RC columns under cyclic loading”, *Steel Compos. Struct.*, **21**(2), 411-427.
- Sundarraja, M.C. and Prabhu, G.G. (2012), “Experimental study on CFST (concrete filled steel tubular) members strengthened by CFRP composites under compression”, *J. Constr. Steel Res.*, **72**(5), 75-83.
- Teng, J.G., Chen, J.F., Smith, S.T. and Lam, L. (2002), *FRP-Strengthened RC Structures*, John Wiley & Sons, Ltd., New York, U.S.A.
- Teng, J.G., Zhao, J.L., Yu, T., Li, L.J. and Guo, Y.C. (2012), “Recycling of coarsely-crushed concrete for use in FRP tubular columns”, *Proceedings of the 1st International Conference on Performance-Based and Life-Cycle Structural Engineering*, Hong Kong, China, December.
- Vanaja, A. and Rao, R.M.V.G.K. (2002), “Fibre fraction effects on thermal degradation behaviour of GFRP, CFRP and hybrid composites”, *J. Reinf. Plast. Compos.*, **21**(15), 1389-1398.
- Xu, S.D. (2012), “Study on mechanical properties of concrete circular column confined by HFRP under axial compression”, M.S. Dissertation, Guangdong University of Technology, China.
- Zhao, J.L., Teng, J.G., Yu, T. and Li, L.J. (2013), “Experimental behavior of FRP-concrete-steel double-skin tubular beams”, *Proceedings of the 11th International Symposium on Fiber Reinforced Polymers for Reinforced Concrete Structures*, Guimarães, Portugal, June.

CC